Composites Part B 167 (2019) 387–395

Contents lists available at ScienceDirect

Composites Part B

journal homepage: www.elsevier.com/locate/compositesb

Phenyl silane treatment and carding process to improve the mechanical, thermal, and water-absorption properties of regenerated cellulose lyocell/polylactic acid bio-composites

Ji-Won Park[a,b], Tae-Hyung Lee[a], Jong-Ho Back[a], Seong-Wook Jang[a,b], Hyun-Joong Kim[a,b,*], Mikael Skrifvars[c]

[a] The Lab of Adhesion and Bio-Composite, Program in Environmental Materials Science, Department of Forest Science, Seoul National University, Seoul 08826, Korea
[b] Research Institute of Agriculture and Life Sciences, Seoul National University, Seoul 08826, Korea
[c] Swedish Centre for Resource Recovery, Faculty of Textiles, Engineering and Business University of Borås, SE-501 90, Borås, Sweden

ARTICLE INFO

Keywords:
Lyocell
Polylactic acid (PLA)
Phenyl silane
Hydrophobic treatment
Carding process
Composite orientation

ABSTRACT

We fabricated a new composite material with increased lyocell (a form of rayon that consists of cellulose fiber made from dissolving wood pulp) content through a surface hydrophobic treatment using phenyl silane and fiber carding/melt pressing. A matrix of polylactic acid (PLA) was used to enhance the environment-friendly properties of the composite and a carding process was used to orient the fibers in the composite. The lyocell content was controlled from 10% to 90%. Cross direction (CD) and machine direction (MD) samples were prepared to confirm the effect of the fiber directionality of the composite on its mechanical properties. The MD samples performed better than the CD samples. The tensile, flexural, and impact strengths of the composite were increased by approximately 85%, 155%, and 55%, respectively, after surface treatment. In the heat-resistance evaluation, confirmed by pyrolysis, surface treatment showed an average improvement of more than 10 °C. The water-absorption characteristics showed dramatic improvement, with enhanced surface-wetting properties and excellent initial moisture-absorption properties in the immersion test. Based on the comprehensive results, we conclude that the performance of the composite was satisfactory even when the content of lyocell was 50% or more.

1. Introduction

In response to the increased concern regarding global environmental issues, green composite materials utilizing bioplastics are becoming popular as substitutes for petroleum-based polymeric materials that are difficult to recycle and disintegrate [1–3]. Among these, natural fiber reinforced polymers (NFRP) are composite materials that utilize natural fibers and biodegradable polymers or nonbiodegradable polymer resins as a matrix. They are also referred to as bio-composite materials when a matrix having some biodegradability or complete biodegradability and environment-friendly reinforcing fibers, called bio-fibers, are used [4,5]. In the initial stages of research on bio-composites, materials that have eco-friendliness and can maintain mechanical strength were investigated. In recent years, however, bio-composites have been studied not only as environmentally friendly materials but also as materials having various functions [2]. For example, lightweight foam structural materials that are used as the main walls of electrical and electronic packaging and transportation equipment have been developed based on bio-composites, as well as conductive substrate materials for next-generation devices [6–8].

The core material that constitutes natural fibers is cellulose. Cellulose is one of the most abundant living resources on the planet. However, the cellulose present in nature is difficult to use directly. Cellulose does not exist alone; it mostly exists in combination with other compounds such as lignin or hemicellulose. Various chemical techniques have recently been introduced, for separating cellulose from the biomass. For example, lyocell is a type of artificial cellulose fiber produced by an environment-friendly process, and has low toxicity

---

Abbreviations: PLA, polylactic acid; CD, cross direction; MD, machine direction; NFRP, natural fiber reinforced polymers; NMMO, *N*-methylmorpholine-*N*-oxide; PTMS, phenyltrimethoxysilane; TGA, thermal gravimetric analysis; FE-SEM, field-emission scanning electron microscopy

[*] Corresponding author. The Lab of Adhesion and Bio-Composite, Program in Environmental Materials Science, Department of Forest Science, Seoul National University, Seoul 08826, Korea.

E-mail address: hjokim@snu.ac.kr (H.-J. Kim).

https://doi.org/10.1016/j.compositesb.2019.02.064
Received 24 December 2018; Received in revised form 14 February 2019; Accepted 26 February 2019

levels during the manufacture, handling of *N*-methylmorpholine-*N*-oxide (NMMO), and biodegradation [9,10]. Another advantage is that the fiber surface is cleaned during the NMMO handling process, and therefore, various surface treatments can be performed easily. Therefore, the potential for utilizing lyocell as an NFRP fiber filler is high [11,12].

Polylactic acid (PLA) is a typical naturally derived polymer and is the most popular material currently used in the industry. Research on fiber-reinforced composites is being actively carried out in order to expand the possibility of using PLA as a matrix component. In particular, various studies have been conducted to improve the brittleness of PLA. Based on these studies, PLA-based composites have been researched as automobile interior materials that require excellent mechanical strength [5,13]. Composite materials using PLA and lyocell fiber reinforcements have recently been developed, and excellent performance improvements have arose from using lyocell as a fiber reinforced [14–16].

Composite fabrication technology using fiber spinning and press melting techniques has various advantages. By controlling the fiber directionality of the composite material, excellent strength can be realized in a specific direction [17–19]. In addition, since the damage to the fiber filler can be minimized during fabrication, the performance degradation of the fiber is almost negligible. Moreover, since long fibers can be used directly, excellent strength reinforcement effects can be expected in the fiber direction. Finally, the ratio of the matrix to the filler can be controlled flexibly and the filler content can be maximized.

Cellulose-based fibers are hydrophilic, which is a disadvantage when they are utilized in a composite material [12,20]. When the composite material absorbs moisture, the internal structure of composites swells, resulting in structural instability. In addition, this hydrophilicity promotes the hydrolysis of the PLA matrix in the composites, further reducing the stability of the composite material. Various research groups have tried to solve these problems caused by the moisture-binding characteristics, by strengthening the bonding force between the matrix and the filler, reducing the penetration route of water, or by surface treatment [21–23].

Among such strategies, the silane surface treatment is a technique that has been widely utilized because this process is easy to handle and can be applied to a wide range of materials. This treatment has the advantage of selectively controlling the surface functional groups during the surface treatment process [24]. For composites using cellulose reinforcements, researchers have attempted to strengthen the bonding force between cellulose and the matrix by utilizing silanes with an acrylate, epoxy, amino or alkyl structure [25,26]. On the other hand, phenyl and thiol structures have mainly been used to control the surface of nanoparticle reinforcements or to enhance their photoreactivity [27,28].

In this study, the surface of lyocell fibers was treated to maximize the content of lyocell while enhancing the mechanical strength, thermal properties, and water resistance. The surface of the lyocell was reformed as a water-repellent surface using phenyltrimethoxysilane (PTMS), and a nonwoven fabric with directional properties was fabricated through fiber spinning and carding with fiberized PLA. The composites were fabricated by melting/hot pressing the fabricated nonwoven fabric. The properties of the composites were analyzed in various ways, according to the content and manufacturing direction of the lyocell. Through this approach, we confirmed that we could increase the lyocell content via fiber processing, and at the same time, we confirmed the possibility of manufacturing a composite material with excellent mechanical performance, heat resistance, and water resistance.

2. Experimental

2.1. Materials

The PLA fiber supplied by Huvis (Republic of Korea) was used as the matrix. The density of the PLA fiber was 1.24 g/cm^3, and its average length was 52 mm. Lyocell fiber (Tencel Lenzing Lyocell, 1.7 dtex, 30 mm cut length) was supplied by Lenzig AG, Business Development and Innovation Textiles in Austria, and was used for reinforcement. PTMS (OFS-6124 XIAMETER®, Dow Corning Toray Co., Ltd., USA) supplied by Yuchang FC was used to make the surface of the lyocell fiber hydrophobic.

2.1.1. Fiber surface treatment

PTMS was used as a coupling agent. To treat the lyocell surface, 0.5 wt% silane was dissolved for hydrolysis in methanol and then lyocell fibers are soaked in solution for two minutes at 25 °C by agitating continuously. Finally, the lyocell fibers were dried in an oven at 110 °C for 10 min. During the reaction in methanol, the methoxy functional groups of PTMS are replaced by hydroxyl groups, and the resulting substituted structure is hydrogen bonded to the cellulosic hydroxyl groups on the lyocell surface. At this time, if the ambient temperature is increased, the hydroxyl groups in the modified PTMS bond to those on the lyocell surface via a condensation reaction. During this process, the hydroxyl structure of PTMS is not only fixed onto the lyocell surface but also forms a continuous layer on this surface as bonding proceeds (Fig. 1). Finally, a cellulose fiber coated with a phenyl structure is obtained, and the chemical, mechanical and electrical properties of the surface are changed.

2.1.2. Carding and needling of the lyocell fiber

An overall schematic diagram of the composite material manufacturing process using PLA and lyocell is shown in Fig. 2. The lyocell fiber was carded and needled to obtain a nonwoven mat. A bale opener was used to separate the fibers (lyocell and PLA) from the bulk. The fibers were mixed according to the lyocell to PLA weight ratios of 1:9, 3:7, 5:5, 7:3, and 9:1 using a bale opener before being fed into the carding machine. A cylindrical cross-lap machine supplied by Cormatex (Prato, Italy) was used for carding the fibers according to the ratio. The cellulose fibers were separated manually and fed into the carding machine. The frequency of the trolley was 40 Hz, which was equivalent to 7.5 m/min, at the outlet. The needling machine was supplied by Certec, Sourcieux-les-Mines, France. The needle punching was done at a frequency of 200 cp/min and the feeding rate was 1.5 m/min, while the

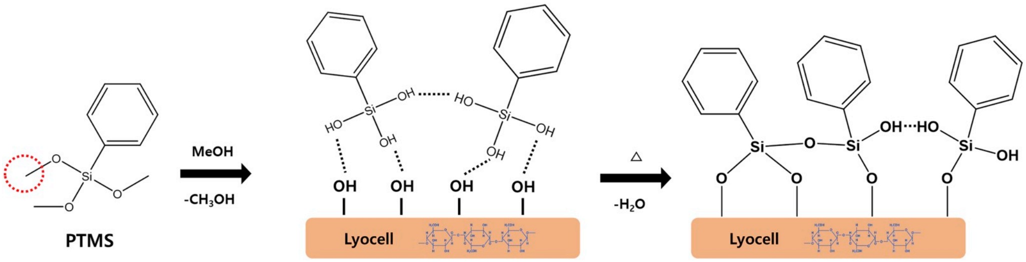

Fig. 1. Surface treatment of lyocell using phenyl silane.

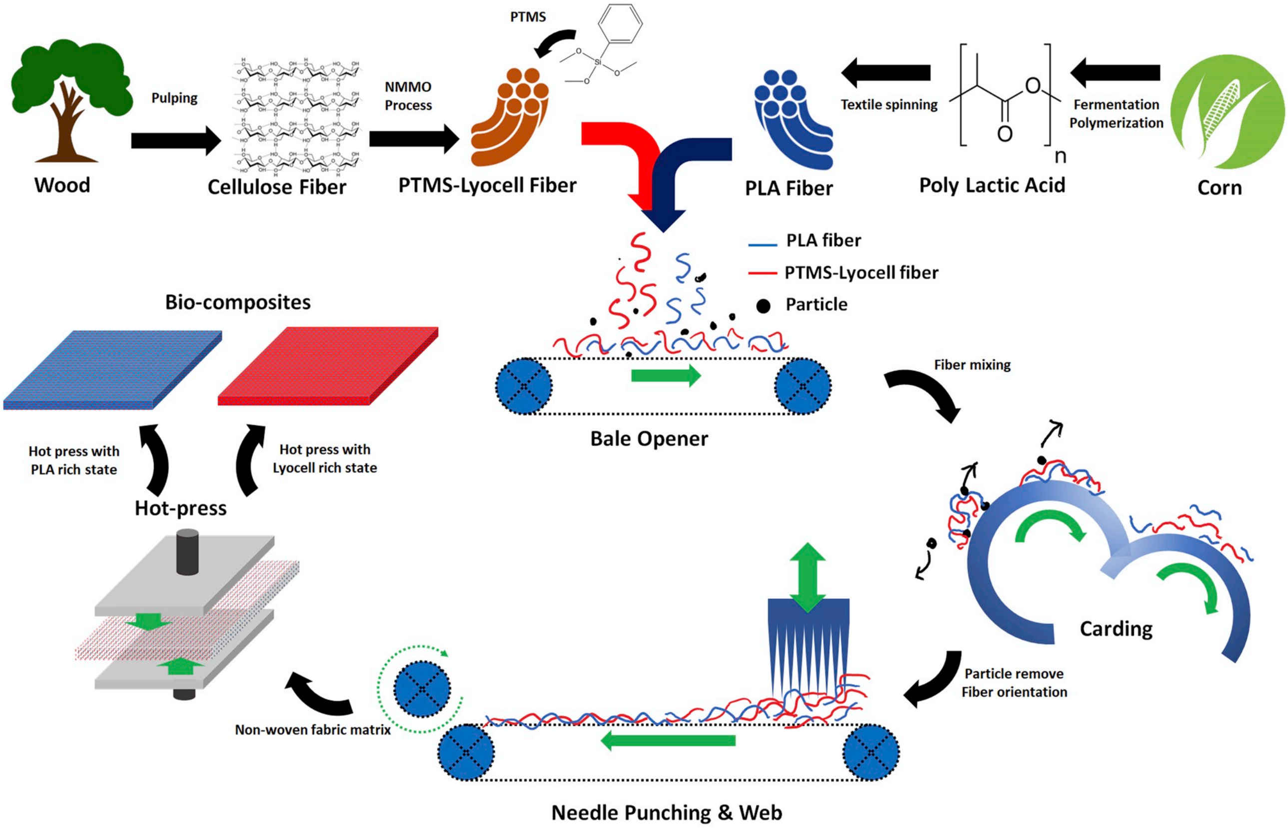

Fig. 2. Manufacturing process of lyocell/PLA composite material, including the carding/melt press process.

depth of the needle was 8 mm.

2.1.3. *Composite fabrication*

The bio-composite of PLA/lyocell was prepared using a carding machine. After preparing composites by the carding process, they were finished by hot pressing at 180 °C for five minutes at 980.6 MPa.

2.2. *Test methods*

2.2.1. *Measurement of mechanical strength according to the fiber orientation*

The tensile, flexural, and impact strengths, which are mechanical properties of composites, show different tendencies depending on the types of matrix and filler components in the composites and their bonding structures. In addition, the composites produced in this study exhibit fiber directionality owing to the carding process. This directionality is a major factor affecting the mechanical properties [18,29]. Therefore, to measure the mechanical properties, two types of samples were prepared, namely, cross-direction samples (CD, wherein the fibers generated in the carding process are oriented orthogonally to the orientation of the tensile test specimen) or machine-direction samples (MD, wherein the fibers generated by carding are oriented in the same direction as the orientation of the tensile test specimen).

2.2.2. *Tensile & flexural strength*

Tensile and flexural specimens were measured using a universal testing machine (Zwick Co, Germany) by ASTM D 638–10 and ASTM D 790–10. The cross speed of the machine during measurement was 5 mm/min, and the mechanical properties were analyzed at room temperature. Six specimens were measured to calculate the margin of error.

2.2.3. *Izod impact test*

The un-notched Izod impact strength tests were conducted at room temperature. Each value obtained represented the average of five samples.

2.2.4. *Thermal gravimetric analysis*

Thermal gravimetric analysis (TGA) measurements were conducted with a thermogravimetric analyzer (TGA 4000, Perkin Elmer Life and Analytical Sciences, USA) on samples at temperatures ranging from room temperature to 500 °C at a heating rate 10 °C/min. The samples were measured immediately after they were dried under vacuum and then packed in polyethylene bags to avoid absorption of water molecules. TGA was conducted on specimens placed in high-quality nitrogen (99.5% nitrogen, 0.5 °C oxygen) atmosphere with a flow rate of 19.8 mL/min to avoid oxidation reactions.

2.2.5. *Water absorption test on the composites*

Rectangular specimens (35 × 12 × 3 mm) were used in the water-absorption test. The samples were immersed in distilled water at room temperature. During testing, the samples were removed from the water, patted dry, and their mass change was recorded with an electronic balance. The water absorption of the composites was calculated as the weight difference and reported as the percentage increase with respect to the initial weight.

2.2.6. *Field emission-scanning electron microscopy*

To determine how the binding characteristics between fibers change, the cross-section of the fracture test specimens was analyzed after the tensile strength test. Field emission-scanning electron microscopy (FE-SEM, SUPRA 55VP, Carl Zeiss, Germany) was conducted at an accelerating voltage of 10 kV, to observe the morphology of the composites consisting of lyocell and PLA. All samples were precoated with a homogeneous platinum layer (purity, 99.99%) by ion sputtering,

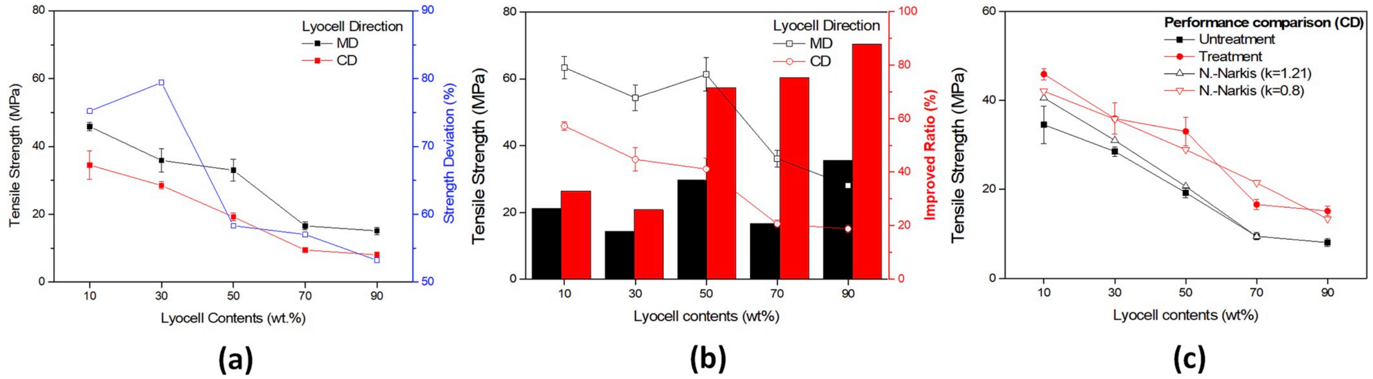

Fig. 3. Results of tensile strength for different orientations: (a) untreated composites, (b) treated composites, (c) comparison with expected properties from N.-Narkis modeling in the cross direction.

to eliminate electron charging before the measurement.

3. Results & discussion

In the tensile-strength test (Fig. 3), the strength tends to decrease steadily as the weight fraction of lyocell increases. In addition, the composite with a CD structure exhibits weaker overall strength than the composite with the MD structure, which was expected. The strength ratio between directions was calculated using the following equation, to analyze the intensity change depending on the directionality.

$$\text{Strength Deviation (\%)} = \frac{\text{Tensile strength in CD structure}}{\text{Tensile strength in MD structure}} \times 100 \tag{1}$$

As the content of lyocell increases, the difference in strength with respect to directionality increases; thus, the difference in the mechanical properties that depend on the direction also increases. When the content of lyocell is 10%, the strength deviation is 75%, and when the content of lyocell is 90%, it is decreased to 53% (Fig. 3-(a)). This result suggests that the binding force between fibers in the CD has a greater influence than those in the MD. Therefore, the performance of the composite material should be analyzed from a different viewpoint depending on the fiber orientation. When the weight ratio of lyocell is low, the fiber-reinforced effect is due to the MD fiber reinforcements. The effect of fiber reinforcement on the fiber composite system can be predicted by the following equation [30],

$$F_{composites} = F_{fib}V_{fib} + F_m(1 - V_{fib}) \tag{2}$$

where F_{fib} is the tensile strength of the fiber, V_{fib} is the volume fraction of the fiber, and F_m is the tensile strength of the matrix. The PLA and lyocell fibers have tensile strengths of approximately 45 MPa and 250 MPa, respectively. Based on this model, the MD tensile strength is predicted to be 65.5 MPa. The experimental result is 50.1 MPa, which does not reach the theoretical predictions but shows enhanced results compared to that of the existing PLA fibers. However, in the case of the CD structure, the strength tends to decrease to 34.5 MPa. The Nicolais & Narkis model predicts the strength of a composite when the reinforcement is in particle form as [31],

$$F_{composites} = F_m(1 - K \times V_{fib}) \tag{3}$$

Under the condition that there is no coupling interaction force between the particles and the matrix ($k = 1.21$), the obtained results according to the model are very similar to the experimental results (Fig. 3-(c)) [32]. Thus, for samples subject to the carding process, the different models for predicting the composite's strength are applicable, depending on the direction. The surface-treated lyocell(Fig. 3-(b)) shows an excellent strength improvement effect in both the MD and CD structures. The strength improvement before and after the surface treatment was defined as the 'improved ratio' and was derived using the following formula,

$$\text{Improved Ratio (\%)} = \frac{\text{Tensile Strength}_{\text{Treat}} - \text{Tensile Strength}_{\text{untreat}}}{\text{Tensile Strength}_{\text{untreat}}} \times 100 \tag{4}$$

Some points to be noted here are 1) the tensile strength is improved to the same level as that of the predicted model when the content of lyocell is 10%, and 2) the overall strength improvement effect is greater in the CD-oriented composites. This performance improvement can be attributed to the phenyl structure of the modified lyocell surface. First, the strength improvement effect in the MD is expected to be due to the energy transferred between the fiber and the matrix owing to the coupling strength between the phenyl structure and the PLA matrix. This can be interpreted as a result similar to the performance improvement of the composite material due to the general fiber modification. On the other hand, the performance improvement in the CD-oriented composites can be attributed to the influence of the pi–pi bond interactions between phenyl structures on the lyocell surface. When the content of lyocell is 90%, the volume fraction of PLA is only 12%. Therefore, there are regions in the bulk composite where there is no binder PLA resin between the lyocell fibers. At this interface, the phenyl structure induces strong bonds between each lyocell fiber in direct contact. According to the mutual coupling force, a relatively large strength improvement effect is generated in the CD. This tendency also affects the constants for the Nicolais & Narkis model predictions. The results of the new model assuming $k = 0.8$ are similar to those of surface-treated composite materials. The reduction in 'a' implies an increase in the interfacial interaction. Although this specimen is a fiber-based composite, a model that assumes particle-type reinforcements can be applied.

Fig. 4 shows the flexural strength measurement results. Evidently, the strength decreases linearly with the lyocell content in both the MD and CD structures. When there is no interfacial bonding between the PLA and the lyocell, the lyocell acts as a very weak component during bending (Fig. 5). Therefore, as the content of lyocell increases, the volume fraction of PLA decreases, and the strength decreases proportionally. However, the flexural strength is greatly increased by using surface-modified lyocell fibers, and it is confirmed that the strength of the MD structure increases by more than 100% and that of the CD structure increases by more than 150%. In particular, it can be seen that the flexural strength is maintained at a certain level even when the content of lyocell is increased up to 70% in the MD-oriented composites. These results can be interpreted as a result of the increase in the bonding strength with PLA due to the introduction of the phenyl structure and the increase in the shear strength with the improvement of the bonding force between the fibers due to the pi–pi bond [33,34].

Fig. 6 shows the impact strength measurement results. Fillers can have two opposing effects in the growth of cracks. They can also serve

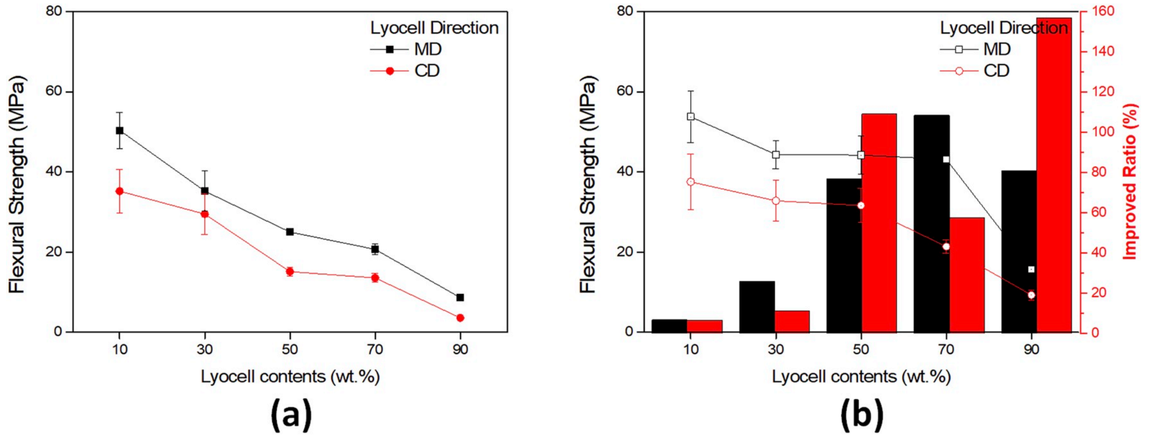

Fig. 4. Results of flexural strength for different orientations: (a) untreated and (b) treated composites.

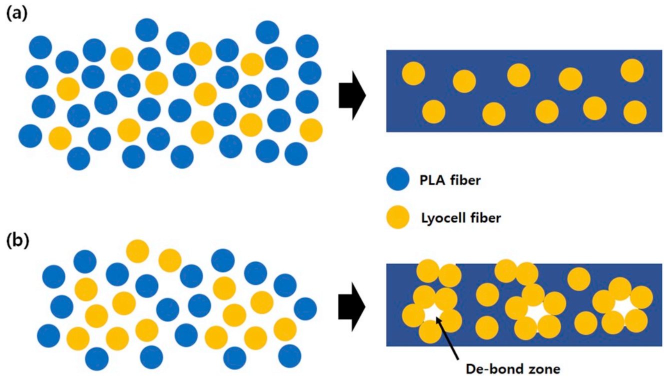

Fig. 5. Composite structural change according to the fiber ratio: (a) PLA-rich and (b) lyocell-rich composites.

as a starting point for crack initiation and can increase the impact strength by lengthening the crack growth route (Fig. 7-(a)). As the composition of the matrix of lyocell and PLA is changed, the impact strength changes greatly and it tends to increase from the initial 2.5 MPa–7 MPa, which is stronger after PTMS treatment.

PLA is a very brittle polymer and is therefore vulnerable to impact. When the content of lyocell is low, the change in the impact strength is not large as the crack grows in the PLA matrix. However, as the content of lyocell increases, the composite's structure changes as less of the PLA matrix is distributed around the reinforcing fiber (Fig. 7-(b)). With the lyocell network as a discontinuous phase, the PLA acts as a continuous binder matrix to create an enhanced network structure. This network structure is very effective in transmitting impact energy. The network becomes stronger as the cohesion of the lyocell and PLA is improved by the PTMS treatment. However, when the amount of PLA is reduced greatly compared to that of the lyocell, the impact strength decreases sharply because the lyocell structure cannot be bound sufficiently.

Through the evaluation of mechanical properties, it was confirmed that the PTMS surface treatment improved the performance by approximately 85%, 155%, and 55% in tensile strength, flexural strength, and impact strength, respectively, which means that the bonding strength between lyocell and PLA was improved through PTMS treatment. In order to confirm the bond structure between the two materials, the fracture profile of the composite with PLA and lyocell mixed in a 1:1 ratio was checked after the tensile test (Fig. 8) via FE-SEM. In the fracture surface of the MD structure (Fig. 8-(a)), the fibers were protruding at the surface, and in the fractured surface of the CD structure (Fig. 8-(b)), the fibers were laid sideways. The structures of these fibers after PTMS treatment were shortened and almost eliminated when broken. This tendency can be confirmed more reliably by enlarging the fracture surface of the CD structure (Fig. 8-(c)). Before the surface treatment, the fibers were elongated, and the PLA was separated from the fiber surface. However, after the PTMS treatment, these fibers were broken, and the PLA was fixed on the lyocell surface. It can be confirmed that the mechanical strength enhancement is manifested by such structural bonding properties.

The pyrolysis characteristics of the lyocell composites showed completely different tendencies when the lyocell content varied from a low to high ratio (Fig. 9). In Fig. 9-(a), the pyrolysis characteristics before and after the surface treatment are compared with those of a

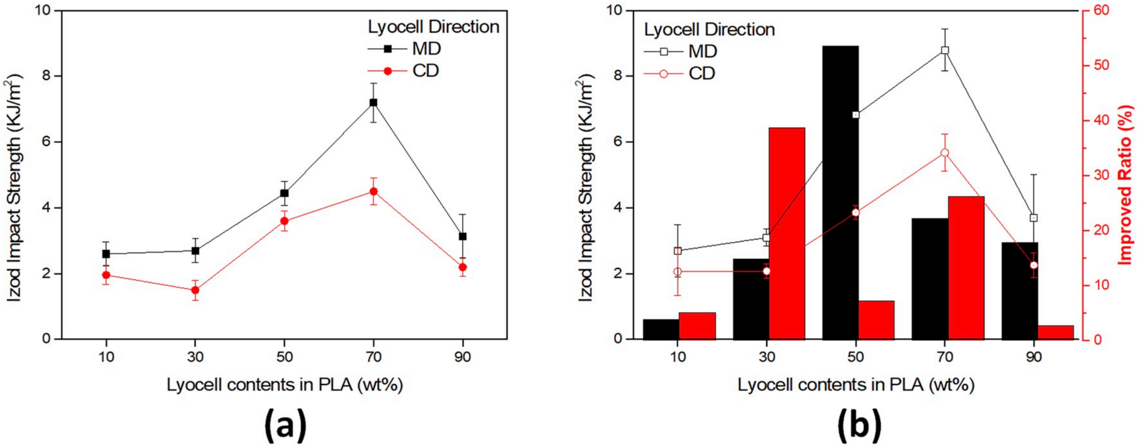

Fig. 6. Impact strength results for different orientations: (a) untreated and (b) treated composites.

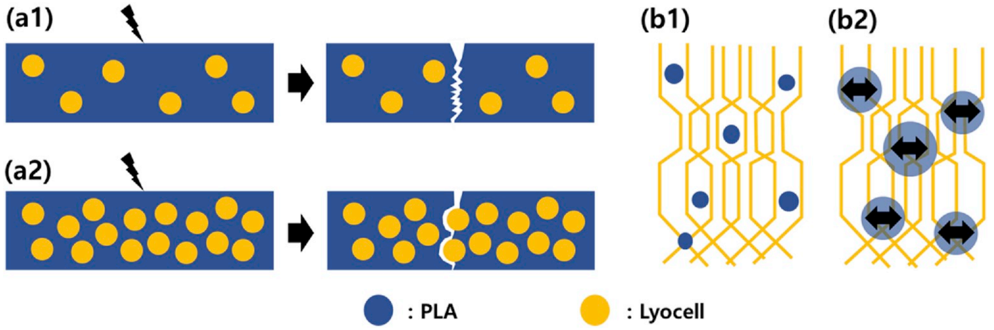

Fig. 7. Impact strength changes according to the content of filler (a) PLA-rich composite, a1: small filler, a2: large filler; (b) lyocell-rich composite, b1: small matrix, b2: large matrix.

composite with lyocell content 10% and 90%, respectively. When the content of lyocell is 90%, there is no change in the pyrolysis curve, according to the surface treatment. The initial decomposition temperatures D_5 and D_{10} of pure PLA are 305.8 and 319.5 °C, respectively. However, the initial decomposition temperature of the composite tends to be lower. Before and after the surface treatment, D_5 was 272.5 and 273.5 °C, and D_{10} was 302.5 and 304.4 °C, respectively (Fig. 9-(b), (c)). The reason for this difference of over 30 °C in the initial decomposition temperature was the decomposition characteristics of the lyocell. Lyocell showed a weight loss that was relatively fast compared to that of cellulose, according to the NMMO process, which is due to dehydration and decomposition of the cellulose [35]. After 380 °C, an ash line that is not found in the pure PLA, was identified. This is the result of the carbide formed by the decomposition of the lyocell.

When the lyocell content is 10%, the thermal stability improvement effect is confirmed by the fiber-reinforcing effect. Before and after the surface treatment, D_5 is 317.3 and 330.4 °C and D_{10} is 332.8 and 342.7 °C, respectively. This indicates that the initial decomposition temperature tends to rise up by 25 °C or more, contrary to the case where the content of lyocell is large. In the structure, in which PLA covers all of the lyocell, hydrogen bonding proceeds at the interfaces. This structural combination serves to enhance the thermal stability of the entire system. In addition, the stability of PLA increases as the hydroxy structure formed during the decomposition bonds with the lyocell more strongly. The phenyl structure formed on the surface through the PTMS treatment enhances the thermal stability of the whole system. The phenyl structure stabilizes the radicals formed during decomposition and strengthens the lyocell and PLA interaction, thus enhancing the structural stability. As a result, the PLA/lyocell composite shows positive synergies, with a higher thermal stability in composite form than each component's respective pyrolysis properties. We have also found that PTMS surface treatment can maximize the effectiveness of this synergy.

Through the PTMS surface treatment, the surface of the lyocell has a hydrophobic structure. The contact angles of the PLA/lyocell composites were measured to investigate the change in surface properties (Fig. 10). In the lyocell composites without surface treatment, we cannot measure the contact angle, except for the composites with a lyocell content of 10% because the liquid droplet is absorbed too quickly and does not maintain a stable shape. The instability at the interface between lyocell and PLA creates pores, which cause water to be absorbed. The water absorption can be calculated using the following formula,

$$\text{Absorption Rate}\left(\frac{uL}{s}\right) = \frac{7.4uL}{\text{The time until the contact angle becomes '0'}} \tag{5}$$

When the content of lyocell was higher than 30%, it was confirmed that more than 4 μL was absorbed per second, which means that the lyocell composite may be vulnerable to initial moisture. Moreover,

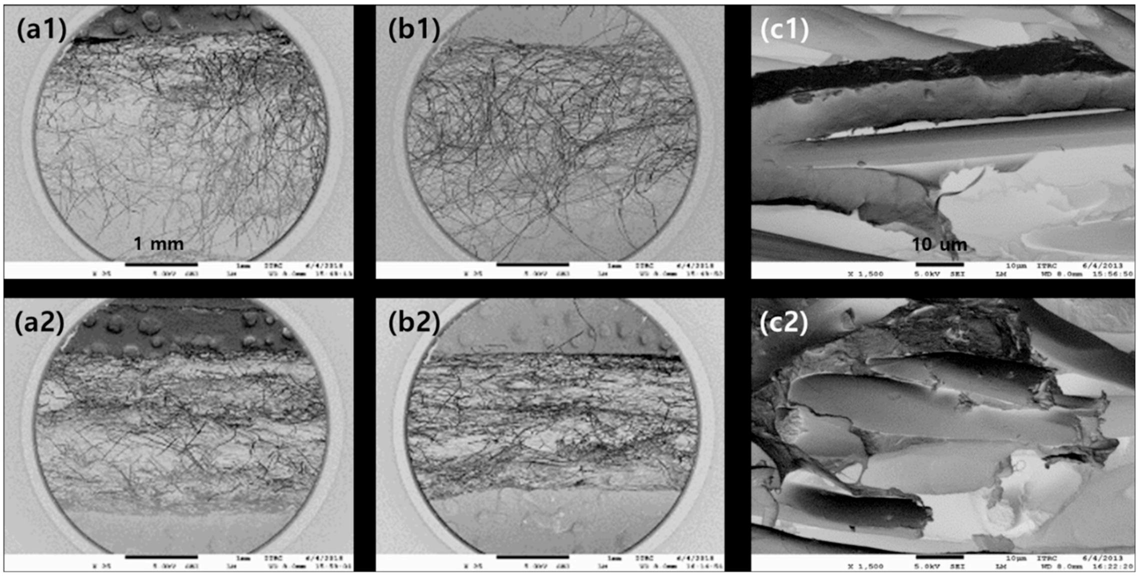

Fig. 8. Field emission-scanning electron microscopy (FE-SEM) images of the tensile fracture surfaces of a bio-composite where the ratio of PLA and lyocell is 50:50. (a1) untreated MD, (a2) silane-treated MD, (b1) untreated CD, (b2) silane-treated CD. The images were magnified 25 times, and the scale bar represents 1 mm. (c1) untreated CD, (c2) silane-treated CD. The images were magnified 1000 times, and the scale bar represents 10 μm.

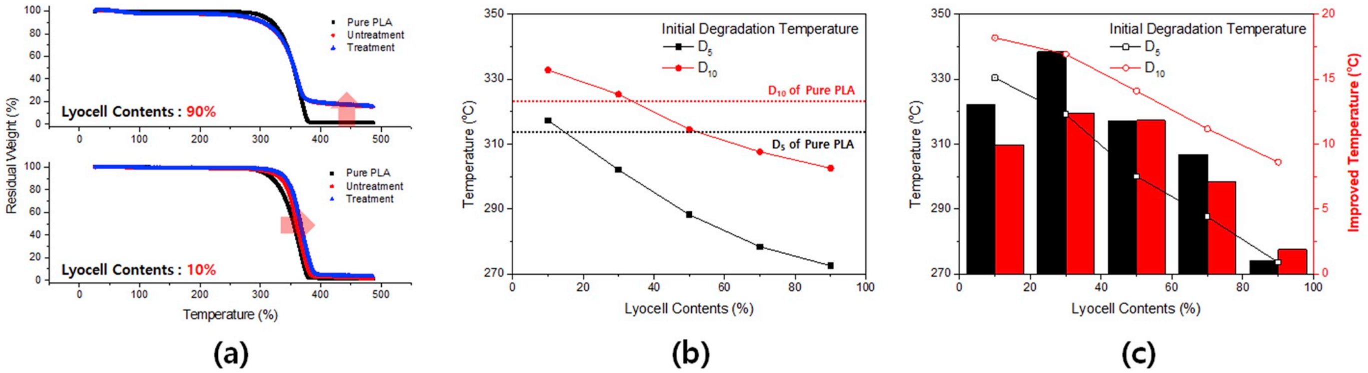

Fig. 9. Heat-resistance evaluation results. (a) Comparing the changes in pyrolysis curves according to the lyocell content. (b) Untreated composites, (c) treated composites.

dramatically improved water absorption properties were observed following the PTMS surface treatment. First, even when the content of lyocell was increased, the water at the surface was not absorbed into the center, and even when the content of lyocell was 90%, it could be confirmed that it was absorbed at a rate of 20 times or slower. When the content of lyocell was increased, the contact angle tended to increase up to 114°. It can be understood that this effect is enhanced when the lyocell is exposed at the composite surface, thereby forming an irregular structure on the surface.

The changes in the properties at the surface also affected the moisture absorption rate of the composite (Fig. 11). Moisture absorption affects the swelling of the material, which not only affects the structural stability negatively but also acts as a factor of hydrolysis. There is no resistance to moisture absorption on samples with no PTMS surface treatment. When the content of lyocell is 10% and 30%, the water uptake tends to increase with time, but when it exceeds 50%, most of the water is absorbed immediately after immersion, and the composite with high lyocell content becomes very vulnerable to moisture. However, PTMS surface treatment shows that these properties are improved very effectively. The initial absorption rate tends to decrease, and it decreases by more than 70% when the lyocell content is 90%. When the content of lyocell is increased, the bonding structure between the fibers is increased, the pores are stretched, and moisture cannot be prevented from entering the pores. However, low wettability due to surface treatment effectively increases this water-absorption time. Finally, although the decrease in the total water absorption ratio is not large, it is confirmed to be very effective in controlling the absorption rate.

4. Conclusion

In summary, a phenyl silane surface treatment enabled increasing the content of lyocell up to 90% and improved the mechanical strength, heat resistance, and water resistance of composites, under all conditions. The tensile strength, flexural strength, and impact strength of the composite materials were improved by approximately 85%, 155%, and 55%, respectively, by the surface treatment. The heat resistance and wetting properties against water were improved by the phenyl silane structure. The carding process was able to direct the orientation of the composite material. The orientation of the composite material was found to have a great influence on the mechanical properties. The physical properties in the MD were superior to those in the CD. This orientation can be effectively utilized in the design of structural composites. The overall results showed that the performance of the composite material was satisfactory even when the content of lyocell was 50% or more. This shows that the filler content of the conventional composite system can be improved greatly. Moreover, the possibility of using various fiber materials is also increased. The best advantage of the fiber carding/melt pressing process used to make composites in this study is the ability to utilize long fibers. If the long fiber is used as it is, the composite can be imparted with a directionality, and an improvement in the mechanical strength can be expected owing to the long fiber. However, since composites are generally manufactured via extrusion, the utilization of long fibers is limited. In contrast, the technique in this study is shown to enable the fabrication of a green composite material that can be utilized for a system requiring high strength through. In addition, since the fibrous material can be utilized as it is,

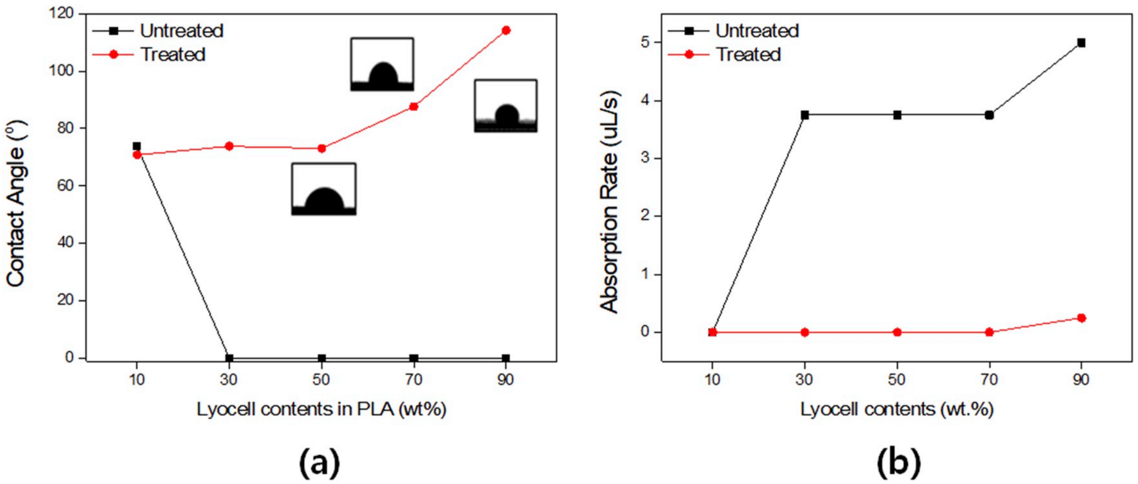

Fig. 10. Evaluation results of surface wettability: (a) contact angle (b) water-absorption time.

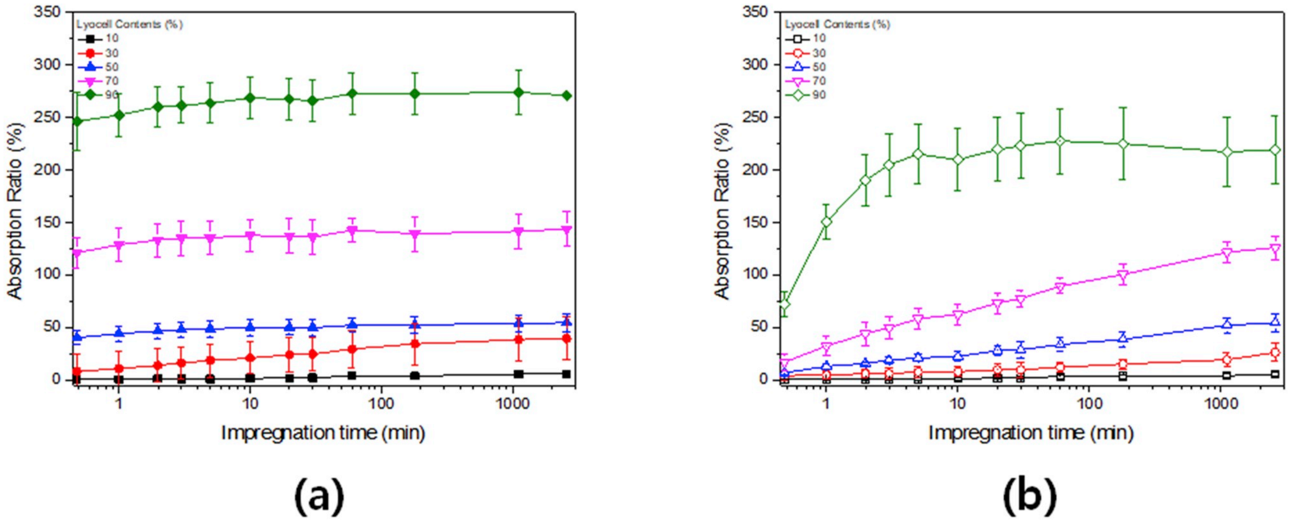

Fig. 11. Evaluation of immersion characteristics with time: (a) untreated composites (b) treated composites.

various regenerated fibers can possibly be applied. Therefore, it is possible to apply this type of fiber to eco-friendly composites through material recycling. In the future, new surface treatment techniques and research findings will be combined to fabricate functional green composite materials.

Acknowledgement

This research was supported by the National Research Foundation of Korea (NRF) and the Swedish Foundation for International Cooperation in Research and Higher Education (STINT) funded by the Ministry of Education, Science and Technology (NRF-2011-0031289).

References

[1] Zhang K, Misra M, Mohanty AK. Toughened sustainable green composites from poly (3-hydroxybutyrate-co-3-hydroxyvalerate) based ternary blends and miscanthus biofiber. ACS Sustainable Chem Eng 2014;2(10):2345–54.

[2] Thakur VK, Thakur MK, Raghavan P, Kessler MR. Progress in green polymer composites from lignin for multifunctional applications: a review. ACS Sustainable Chem Eng 2014;2(5):1072–92.

[3] Ashori A. Wood–plastic composites as promising green-composites for automotive industries!. Bioresour Technol 2008;99(11):4661–7.

[4] Kwon H-J, Sunthornvarabhas J, Park J-W, Lee J-H, Kim H-J, Piyachomkwan K, et al. Tensile properties of kenaf fiber and corn husk flour reinforced poly (lactic acid) hybrid bio-composites: role of aspect ratio of natural fibers. Compos B Eng 2014;56:232–7.

[5] Lee B-H, Kim H-S, Lee S, Kim H-J, Dorgan JR. Bio-composites of kenaf fibers in polylactide: role of improved interfacial adhesion in the carding process. Compos Sci Technol 2009;69(15–16):2573–9.

[6] Cataldi P, Bonaccorso F, Esau del Rio Castillo A, Pellegrini V, Jiang Z, Liu L, et al. Cellulosic graphene biocomposites for versatile high-performance flexible electronic applications vol. 2. 2016. p. 1600245. 11.

[7] Kuang T, Li K, Chen B, Peng XJCPBE. Poly (propylene carbonate)-based in situ nanofibrillar biocomposites with enhanced miscibility, dynamic mechanical properties, rheological behavior and extrusion foaming ability vol. 123. 2017. p. 112–23.

[8] Geng L, Li L, Mi H, Chen B, Sharma P, Ma H, et al. Superior impact toughness and excellent storage modulus of poly (lactic acid) foams reinforced by shish-kebab nanoporous structure vol. 9. 2017. p. 21071–6. 25.

[9] Rosenau T, Potthast A, Sixta H, Kosma P. The chemistry of side reactions and byproduct formation in the system NMMO/cellulose (Lyocell process). Prog Polym Sci 2001;26(9):1763–837.

[10] Rosenau T, Potthast A, Adorjan I, Hofinger A, Sixta H, Firgo H, et al. Cellulose solutions in N-methylmorpholine-N-oxide (NMMO)–degradation processes and stabilizers. Cellulose 2002;9(3–4):283–91.

[11] Johnson RK, Zink-Sharp A, Renneckar SH, Glasser WG. Mechanical properties of wetlaid lyocell and hybrid fiber-reinforced composites with polypropylene. Compos Appl Sci Manuf 2008;39(3):470–7.

[12] Thakur VK, Thakur MK. Processing and characterization of natural cellulose fibers/thermoset polymer composites. Carbohydr Polym 2014;109:102–17.

[13] Kim H-S, Lee B-H, Lee S, Kim H-J, Dorgan JR. Enhanced interfacial adhesion, mechanical, and thermal properties of natural flour-filled biodegradable polymer bio-composites. J Therm Anal Calorim 2010;104(1):331–8.

[14] Soykeabkaew N, Nishino T, Peijs T. All-cellulose composites of regenerated cellulose fibres by surface selective dissolution. Compos Appl Sci Manuf 2009;40(4):321–8.

[15] Thirmizir M, Ishak Z, Taib R, Rahim S, Jani SM. Kenaf-bast-fiber-filled biodegradable poly (butylene succinate) composites: effects of fiber loading, fiber length, and maleated poly (butylene succinate) on the flexural and impact properties. J Appl Polym Sci 2011;122(5):3055–63.

[16] Baghaei B, Skrifvars M. Characterisation of polylactic acid biocomposites made from prepregs composed of woven polylactic acid/hemp–lyocell hybrid yarn fabrics. Compos Appl Sci Manuf 2016;81:139–44.

[17] Gindl W, Martinschitz KJ, Boesecke P, Keckes J. Changes in the molecular orientation and tensile properties of uniaxially drawn cellulose films. Biomacromolecules 2006;7(11):3146–50.

[18] Alavudeen A, Rajini N, Karthikeyan S, Thiruchitrambalam M, Venkateshwaren N. Mechanical properties of banana/kenaf fiber-reinforced hybrid polyester composites: effect of woven fabric and random orientation. Mater Des 2015;66:246–57. 1980-2015.

[19] Quan Z, Wu A, Keefe M, Qin X, Yu J, Suhr J, et al. Additive manufacturing of multidirectional preforms for composites: opportunities and challenges. Mater Today 2015;18(9):503–12.

[20] Toivonen MS, Kurki-Suonio S, Schacher FH, Hietala S, Rojas OJ, Ikkala O. Waterresistant, transparent hybrid nanopaper by physical cross-linking with chitosan. Biomacromolecules 2015;16(3):1062–71.

[21] Nagarajan V, Mohanty AK, Misra M. Sustainable green composites: value addition to agricultural residues and perennial grasses. ACS Sustainable Chem Eng 2013;1(3):325–33.

[22] Shi S, Yang C, Nie M. Enhanced interfacial strength of natural fiber/polypropylene composite with mechanical-interlocking interface. ACS Sustainable Chem Eng 2017;5(11):10413–20.

[23] Ramamoorthy SK, Skrifvars M, Rissanen M. Effect of alkali and silane surface treatments on regenerated cellulose fibre type (Lyocell) intended for composites. Cellulose 2015;22(1):637–54.

[24] Thakur VK, Thakur MK, Kessler MR. Handbook of composites from renewable materials. Functionalization: John Wiley & Sons; 2017.

[25] Wang L, Sanders JE, Gardner DG, Han YJIC. Products. In-situ modification of cellulose nanofibrils by organosilanes during spray drying vol. 93. 2016. p. 129–35.

[26] Qian S. Sheng KJCS, Technology. PLA toughened by bamboo cellulose nanowhiskers: role of silane compatibilization on the PLA bionanocomposite properties vol. 148. 2017. p. 59–69.

[27] Choi MS, Kim HG, Kim BHJBotKCS. Influence of phenylsilane on the textural, structural, and electrochemical properties of activated carbon nanofiber composites vol. 38. 2017. p. 632–5. 6.

[28] Kang T, Jang I, Oh S-GJC, Physicochemical SA, Aspects E. Surface modification of silica nanoparticles using phenyl trimethoxy silane and their dispersion stability in N-methyl-2-pyrrolidone vol. 501. 2016. p. 24–31.

[29] Mortazavian S, Fatemi A. Effects of fiber orientation and anisotropy on tensile strength and elastic modulus of short fiber reinforced polymer composites. Compos B Eng 2015;72:116–29.

[30] Kwon HJ, Sunthornvarabhas J, Park JW, Lee JH, Kim HJ, Piyachomkwan K, et al. Tensile properties of kenaf fiber and corn husk flour reinforced poly(lactic acid) hybrid bio-composites: role of aspect ratio of natural fibers. Compos B Eng 2014;56:232–7.

[31] Park JW, Kim H, Lee JH, Jang SW, Kim HJ. Evaluation of mechanical performance and flame retardant characteristics of biomass-based EVA composites using intumescent flame retardant technology. Journal of the Korean Wood Science and

Technology 2018;46(2):189–201.

[32] Zare Y. “a” interfacial parameter in Nicolais–Narkis model for yield strength of polymer particulate nanocomposites as a function of material and interphase properties. J Colloid Interface Sci 2016;470:245–9.

[33] Bahramian N, Atai M, Naimi-Jamal MR. Ultra-high-molecular-weight polyethylene fiber reinforced dental composites: effect of fiber surface treatment on mechanical properties of the composites. Dent Mater 2015;31(9):1022–9.

[34] Lee H, Ohsawa I, Takahashi J. Effect of plasma surface treatment of recycled carbon fiber on carbon fiber-reinforced plastics (CFRP) interfacial properties. Appl Surf Sci 2015;328:241–6.

[35] Lizundia E, Vilas J, León L. Crystallization, structural relaxation and thermal degradation in Poly (l-lactide)/cellulose nanocrystal renewable nanocomposites. Carbohydr Polym 2015;123:256–65.